

## Tautomerism in the Guanyl Radical

Chrysostomos Chatgililoglu,<sup>\*,†</sup> Clara Caminal,<sup>†,§</sup> Alessio Altieri,<sup>†</sup>  
 Georgios C. Vougioukalakis,<sup>†,||</sup> Quinto G. Mulazzani,<sup>†</sup> Thanasis Gimisis,<sup>†</sup> and  
 Maurizio Guerra<sup>\*,†</sup>

Contribution from the ISOF, Consiglio Nazionale delle Ricerche, Via P. Gobetti 101, 40129  
 Bologna, Italy, and Department of Chemistry, University of Athens, 15771 Panepistimiopolis,  
 Athens, Greece

Received May 3, 2006; E-mail: chrys@isof.cnr.it; guerra@isof.cnr.it

**Abstract:** Despite a few decades of intense study, a full description of tautomers of one-electron-oxidized guanine remains to be achieved. Here we show that two of these tautomers are produced by the protonation of an 8-haloganine electron adduct. The rate constants for the reactions of hydrated electrons ( $e_{aq}^-$ ) with a variety of 8-substituted guanine derivatives have been measured by a pulse radiolysis technique and correlated with both inductive and resonance components of the substituents. The fate of electron adducts was investigated by radiolytic methods coupled with product studies and addressed computationally by means of time-dependent DFT (TD-B3LYP/6-311G\*\*//B1B95/6-31+G\*\*) calculations. The reaction of  $e_{aq}^-$  with 8-haloganosine or 8-halo-2'-deoxyguanosine produces the first observable transient species that decay unimolecularly ( $k = 1 \times 10^5 \text{ s}^{-1}$  at 22 °C) to give the one-electron oxidized guanosine or 2'-deoxyguanosine. Theory suggests that the electron adducts of 8-bromoguanine derivatives protonated at C8 form a  $\pi$ -complex, with the Br atom situated above the molecular plane, that is prompt to eject  $\text{Br}^-$ . The two short-lived intermediates, which show a substantial difference in their absorption spectra, are recognized to be the two purine tautomers (i.e., iminic **7** and aminic **3** forms). The spin density distributions of the two tautomers are quite different at the O6 and N10 positions, whereas they are very similar at the N3, C5, and C8 positions. The resonance structures of the two tautomers are discussed in some detail. B1B95/6-31+G\*\* calculations show also that the tautomerization from the iminic (**7**) to the aminic (**3**) arrangement is a water-assisted process.

## Introduction

The one-electron oxidation of guanosine (**1a**) or 2'-deoxyguanosine (**1b**) has been studied using the powerful  $\text{SO}_4^{\cdot-}$  or the milder  $\text{Br}_2^{\cdot-}$  and  $\text{N}_3^{\cdot}$  oxidants.<sup>1,2</sup> These reactions are thought to involve an electron transfer, giving rise to radical cation **2** (Scheme 1).<sup>3</sup> The reported  $\text{p}K_a$  values of 3.9 and 10.7 are related to the successive deprotonation at N1 and N10 positions, forming radical **3** and radical anion **4**, respectively.<sup>1</sup> A rate constant of  $1.8 \times 10^7 \text{ s}^{-1}$  at pH 7.0 has been measured for the deprotonation reaction **2**→**3**.<sup>6</sup> The main reaction of the  $\text{HO}^{\cdot}$

radical with **1** (65–70%) is the formation of adduct **5** that undergoes a dehydration reaction, with a rate constant of  $6 \times 10^3 \text{ s}^{-1}$  at pH 7, to give **3**.<sup>7</sup> The fate of **3** or **4** under anoxic conditions is not known. In pulse radiolysis experiments **3** decays slowly (ms time scale) and the rate of its hypothetical addition to water is much smaller than that of the bimolecular decay.<sup>7,8</sup> On the other hand, evidence that **2** reacts with water to produce 8-oxo-7,8-dihydro-2'-deoxyguanosine and/or rearranges intramolecularly depending on the substituents has been reported.<sup>9,10</sup>

The EPR/ENDOR study of X-irradiated single crystals of 2'-deoxyguanosine 5'-monophosphate and 3',5'-cyclic guanosine monophosphate at 10 K demonstrated that the radical cation **2** deprotonated immediately after formation at the amino N10 position rather than at N1 to give radical **7**.<sup>11,12</sup> Upon annealing

<sup>†</sup> Consiglio Nazionale delle Ricerche.

<sup>‡</sup> University of Athens.

<sup>§</sup> Present address: Institute for Research in Biomedicine, Barcelona Science Park, Josep Samitier 1, 08028 Barcelona, Spain.

<sup>||</sup> Visiting student from Department of Chemistry, University of Crete (Greece). Present address: Division of Chemistry and Chemical Engineering, California Institute of Technology, Pasadena, California 91125.

(1) (a) Candeias, L. P.; Steenken, S. *J. Am. Chem. Soc.* **1989**, *111*, 1094. (b) Candeias, L. P.; Steenken, S. *J. Am. Chem. Soc.* **1992**, *114*, 699.

(2) Faraggi, M.; Klapper, M. H. *J. Chim. Phys., Phys.-Chim. Biol.* **1994**, *91*, 1062.

(3) The reduction potential of one-electron oxidized guanosine,  $E_7(\mathbf{3}/\mathbf{1}) = 1.29 \text{ V}$ ,<sup>4</sup> is lower than that of  $\text{SO}_4^{\cdot-}$ ,  $\text{N}_3^{\cdot}$ ,  $\text{Br}_2^{\cdot-}$ , and  $\text{HO}^{\cdot}$  radicals,<sup>5</sup> which means that in principle these species can oxidize guanosine or 2-deoxyguanosine by one-electron transfer.

(4) Steenken, S.; Jovanovic, S. V. *J. Am. Chem. Soc.* **1997**, *119*, 617.

(5)  $E^\circ(\text{SO}_4^{\cdot-}/\text{SO}_4^{2-}) \approx 2.43 \text{ V}$ ,  $E^\circ(\text{Br}_2^{\cdot-}/2\text{Br}^-) = 1.66 \text{ V}$ ,  $E^\circ(\text{N}_3^{\cdot}/\text{N}_3^-) = 1.33 \text{ V}$ ,  $E^\circ(\text{HO}^{\cdot}/\text{HO}^-) = 1.90 \text{ V}$ ; see: Wardman, P. *J. Phys. Chem. Ref. Data* **1989**, *14*, 1637.

(6) Kobayashi, K.; Tagawa, S. *J. Am. Chem. Soc.* **2003**, *125*, 10213.

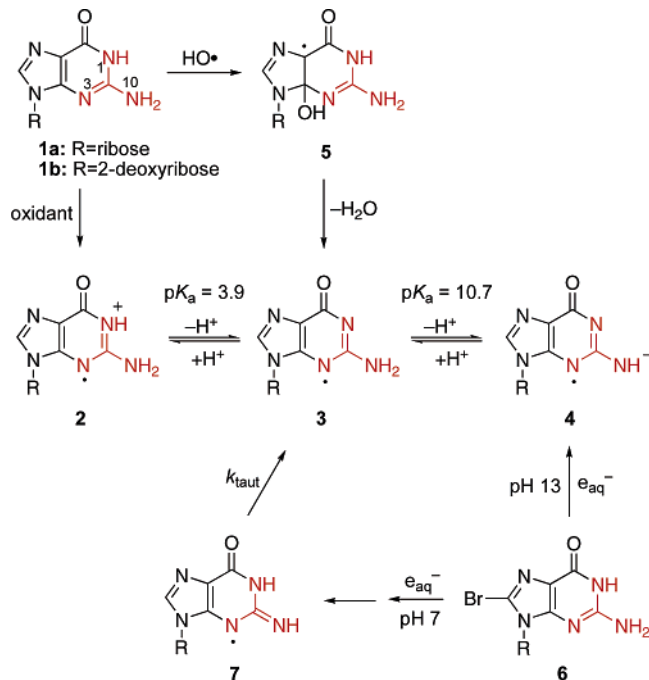
(7) Candeias, L. P.; Steenken, S. *Chem.—Eur. J.* **2000**, *6*, 475.

(8) In the presence of molecular oxygen, the guanine moiety is transformed into five-membered heterocycles, which are thought to be the final products of the addition of **3** to  $\text{O}_2$ . However, the rate constant for this reaction is also expected to be very slow.<sup>7</sup> See: (a) Cadet, J.; Berger, M.; Buchko, G. W.; Joshi, P. C.; Raoul, S.; Ravanat, J.-L. *J. Am. Chem. Soc.* **1994**, *116*, 7403. (b) Raoul, S.; Berger, M.; Buchko, G. W.; Joshi, P. C.; Morin, B.; Weinfeld, M.; Cadet, J. *J. Chem. Soc., Perkin Trans. 2* **1996**, 371. (c) Gasparutto, D.; Ravanat, J.-L.; Gérot, O.; Cadet, J. *J. Am. Chem. Soc.* **1998**, *120*, 10283.

(9) Ravanat, J.-L.; Saint-Pierre, C.; Cadet, J. *J. Am. Chem. Soc.* **2003**, *125*, 2030.

(10) Nakatani, K.; Dohno, C.; Saito, I. *J. Am. Chem. Soc.* **2001**, *123*, 9681.

**Scheme 1.** Radical **3** is a Common Intermediate of the Oxidation of Guanosine **1a** by  $\text{SO}_4^{\cdot-}$  or the Reduction of 8-Bromoguanosine **6** by Hydrated Electrons at pH  $\sim 7$



**7** decayed with no apparent successor above 225 K. Therefore, the site of deprotonation of radical cation **2** is different in the solid state and in an aqueous solution.<sup>13</sup>

The reaction of hydrated electrons ( $\text{e}_{\text{aq}}^-$ ) with 8-bromoguanosine (**6**) was previously studied by us in some detail using pulse radiolysis techniques.<sup>14,15</sup> At pH 13, it was found that this bromide captures electrons and forms radical **4**. At pH 7, these experiments revealed the formation of two short-lived intermediates. We recently suggested that the initial electron adduct is rapidly protonated at the C8 position to give  $\text{Br}^-$ , and the first observable transient species (2  $\mu\text{s}$  after the pulse) was assigned to radical **7**. This species decays by first-order kinetics to produce the one-electron oxidized guanosine **3** via tautomerization. Product studies showed also that 8-bromoguanine derivatives are prone to capture  $\text{e}_{\text{aq}}^-$  with a quantitative formation of the corresponding debrominated nucleosides,<sup>14,16</sup> and therefore, they can be considered as an efficient detection system for excess electron-transfer processes.<sup>17</sup> Indeed, in recent papers 8-bromo-2'-deoxyguanosine was incorporated in a variety of single- or double-stranded oligonucleotides<sup>18,19</sup> and G-quadruplexes,<sup>16</sup> and the reaction with hydrated electrons<sup>16,18</sup> or

light-dependent flavin electron injector<sup>19</sup> indicated that excess electron transfer is effective.

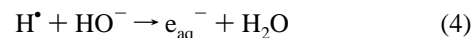
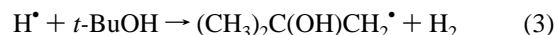
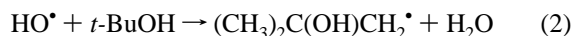
In this article, we report a detailed pulse radiolysis study on the reaction of  $\text{e}_{\text{aq}}^-$  with a variety of 8-substituted guanine derivatives (Chart 1). The identification of various transient species has also been addressed computationally by means of DFT calculations. Our main objective is to obtain a solid background for this paradoxical generation of one-electron oxidized guanine derivatives under reducing conditions and to study in detail the tautomerism between radicals **7** and **3** (see Scheme 1).<sup>15</sup>

## Results and Discussion

**Radiolytic Production of Transients.** Radiolysis of neutral water leads to  $\text{e}_{\text{aq}}^-$ ,  $\text{HO}^\bullet$ , and  $\text{H}^\bullet$  as shown in eq 1. The values in parentheses represent the radiation chemical yields ( $G$ ) in units of  $\mu\text{mol J}^{-1}$ .<sup>20a</sup> The reactions of  $\text{e}_{\text{aq}}^-$  with the substrates



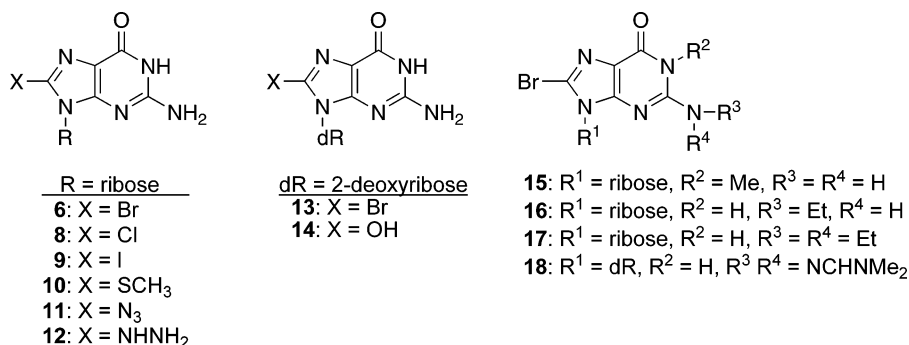
were studied in  $\text{O}_2$ -free solutions containing 0.25 M *t*-BuOH. With this amount of *t*-BuOH,  $\text{HO}^\bullet$  is scavenged efficiently (eq 2,  $k_2 = 6.0 \times 10^8 \text{ M}^{-1} \text{ s}^{-1}$ ),<sup>20</sup> whereas  $\text{H}^\bullet$  is trapped only partially (eq 3,  $k_3 = 1.1 \times 10^6 \text{ M}^{-1} \text{ s}^{-1}$ ).<sup>21</sup> In an alkaline solution, additional  $\text{e}_{\text{aq}}^-$  is produced from the reaction of  $\text{H}^\bullet$  with  $\text{HO}^-$  (eq 4,  $k_4 = 2.2 \times 10^7 \text{ M}^{-1} \text{ s}^{-1}$ ).<sup>20</sup>



**Reactivity of Substituted Guanine Derivatives toward Hydrated Electrons.** The pseudo first-order rate constant,  $k_{\text{obs}}$ , for the reaction of  $\text{e}_{\text{aq}}^-$  with a variety of substituted guanine derivatives (Chart 1) was determined by measuring the rate of the optical density decrease of  $\text{e}_{\text{aq}}^-$  at 720 nm ( $\epsilon = 1.9 \times 10^4 \text{ M}^{-1} \text{ cm}^{-1}$ )<sup>22</sup> at pH  $\sim 7$ . From the slope of  $k_{\text{obs}}$  vs nucleoside concentration, the bimolecular rate constants ( $k$ ) were determined (see Supporting Information). In Table 1 the values for 8-substituted guanosines and 2'-deoxyguanosines are reported.<sup>23,24</sup> The values varied slightly (less than 1 order of magnitude), with the fastest being for  $\text{X} = \text{N}_3$  and the slowest

- (11) (a) Hole, E. O.; Nelson, W. H.; Sagstuen, E.; Close, D. M. *Radiat. Res.* **1992**, *129*, 119. (b) Hole, E. O.; Nelson, W. H.; Close, D. M.; Sagstuen, E. *J. Chem. Phys.* **1987**, *86*, 5218.  
 (12) Hole, E. O.; Sagstuen, E.; Nelson, W. H.; Close, D. M. *Radiat. Res.* **1992**, *129*, 1.  
 (13) It should be emphasized that each of the radicals **2**, **3**, **4**, and **7** has several resonance forms. In radical **7**, for example, the  $\pi$ -spin densities at the N10, N3, and C8 positions are 33%, 31%, and 17.5%, respectively.<sup>11,12</sup> The reported drawings in Scheme 1 are therefore chosen for a facile comprehension and the guanidine moieties are marked in red color.  
 (14) Ioele, M.; Bazzanini, R.; Chatgililoglu, C.; Mulazzani, Q. G. *J. Am. Chem. Soc.* **2000**, *122*, 1900.  
 (15) Chatgililoglu, C.; Caminal, C.; Guerra, M.; Mulazzani, Q. G. *Angew. Chem., Int. Ed.* **2005**, *44*, 6030.  
 (16) De Champdoré, M.; De Napoli, L.; Montesarchio, D.; Piccialli, G.; Caminal, C.; Mulazzani, Q. G.; Navacchia, M. L.; Chatgililoglu, C. *Chem. Commun.* **2004**, 1756.

- (17) For selected recent papers on the excess electron transfer, see: (a) Wagenknecht, H.-A. *Angew. Chem., Int. Ed.* **2003**, *42*, 2454. (b) Carell, T.; Behrens, C.; Gierlich, J. *Org. Biomol. Chem.* **2003**, *1*, 2221. (c) Breeger, S.; Hennecke, U.; Carell, T. *J. Am. Chem. Soc.* **2004**, *126*, 1302. (d) Ito, T.; Rokita, S. E. *Angew. Chem., Int. Ed.* **2004**, *43*, 1839. (e) Giese, B.; Carl, B.; Carl, T.; Carell, T.; Behrens, C.; Hennecke, U.; Schiemann, O.; Feresin, E. *Angew. Chem., Int. Ed.* **2004**, *43*, 1848. (f) T. Ito and S. E. Rokita, *J. Am. Chem. Soc.* **2004**, *126*, 15552. (g) Wagner, C.; Wagenknecht, H.-A. *Chem.-Eur. J.* **2005**, *11*, 1871. (h) Kaden, P.; Mayer-Enthart, E.; Trifonov, A.; Fiebing, T.; Wagenknecht, H.-A. *Angew. Chem., Int. Ed.* **2005**, *44*, 1636. (i) Mayer-Enthart, E.; Kaden, P.; Wagenknecht, H.-A. *Biochemistry* **2005**, *44*, 11749.  
 (18) Kimura, T.; Kawai, K.; Tojo, S.; Majima, T. *J. Org. Chem.* **2004**, *69*, 1169.  
 (19) Manetto, A.; Breeger, S.; Chatgililoglu, C.; Carell, T. *Angew. Chem., Int. Ed.* **2006**, *45*, 318.  
 (20) (a) Buxton, G. V.; Greenstock, C. L.; Helman, W. P.; Ross, A. B. *J. Phys. Chem. Ref. Data* **1988**, *17*, 513. (b) Ross, A. B.; Mallard, W. G.; Helman, W. P.; Buxton, G. V.; Huie, R. E.; Neta, P. *NDRL-NIST Solution Kinetic Database*, version 3; Notre Dame Radiation Laboratory; Notre Dame, IN and NIST Standard Reference Data, Gaithersburg, MD, 1998.  
 (21) Wojnárovits, L.; Takács, E.; Dajka, K.; Emmi, S. S.; Russo, M.; D'Angelantonio, M. *Radiat. Phys. Chem.* **2004**, *69*, 217.  
 (22) Hug, G. L. *Nat. Stand. Ref. Data Ser., Nat. Bur. Stand.* **1981**, *69*, 6.  
 (23) Rate constants of  $6 \times 10^9$  and  $7.4 \times 10^9 \text{ M}^{-1} \text{ s}^{-1}$  have been reported for the reaction of  $\text{e}_{\text{aq}}^-$  with **1a**.<sup>20</sup>

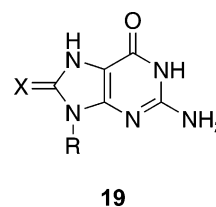
**Chart 1.** 8-Substituted Guanine Derivatives Studied by Pulse Radiolysis in This Work**Table 1.** Rate Constants for the Reaction of e<sub>aq</sub><sup>-</sup> with 8-Substituted Guanine Derivatives in Aqueous Solution at pH ~7

substrate	X	$k/10^{10} \text{ M}^{-1} \text{ s}^{-1}$	$F^a$	$R^b$
<b>1a</b>	H	0.31 ± 0.01	0.03	0.00
<b>1b</b>	H	0.30 ± 0.01	0.03	0.00
<b>8</b>	Cl	0.56 ± 0.01	0.42	-0.19
<b>6</b>	Br	1.1 <sup>b</sup>	0.45	-0.22
<b>13</b>	Br	0.95 ± 0.05	0.45	-0.22
<b>9</b>	I	1.3 ± 0.1	0.42	-0.24
<b>14</b>	OH	0.56 ± 0.01	0.33	-0.70
<b>10</b>	SCH <sub>3</sub>	0.63 ± 0.02	0.23	-0.23
<b>11</b>	N <sub>3</sub>	1.4 ± 0.2	0.48	-0.40
<b>12</b>	NHNH <sub>2</sub>	0.26 ± 0.01	0.22	-0.77

<sup>a</sup> From ref 25. <sup>b</sup> From ref 14.

one for X = NHNH<sub>2</sub>. In Table 1, Swain and Lupton's modified constants for inductive ( $F$ ) and resonance ( $R$ ) effects are also reported in order to correlate the electronic effect of the substituents.<sup>25</sup> For Br, I, and N<sub>3</sub> substituents which show a higher electron-withdrawing power and moderate resonance stabilization, the addition of e<sub>aq</sub><sup>-</sup> was also found to be the fastest one. For the SCH<sub>3</sub> substituent, both inductive and resonance effects are moderate and the reactivity is twice that of guanosine. On the other hand, the highest resonance stabilization given by the NHNH<sub>2</sub> group together with its moderate electron-withdrawing power is associated with a slower e<sub>aq</sub><sup>-</sup> addition process. It is also worth mentioning that compounds **12** and **14** are in equilibrium with their tautomeric forms (see the general structure **19**), and at least in the nucleoside **14** where the 8-oxo form is the main one, these forms should play a part. In summary, both the inductive and resonance components of a substituent X can have a role in the reactivity of 8-substituted guanosines toward hydrated electrons.<sup>26</sup> Rate constants ( $k/10^{10} \text{ M}^{-1} \text{ s}^{-1}$ ) of 1.1 ± 0.2, 0.83 ± 0.04, 0.80 ± 0.02, and 2.2 ± 0.3 were also determined at pH ~7 for the reaction of e<sub>aq</sub><sup>-</sup> with the 8-bromo derivatives **15**, **16**, **17**, and **18**, respectively. Therefore, the alkyl substitution at the NH and NH<sub>2</sub> positions of the guanine moiety did not influence substantially the reactivity toward hydrated electrons.

**Fate of Electron Adducts of 8-Halo Substituted Guanine Derivatives.** The spectral changes obtained from the pulse irradiation of Ar-purged aqueous solutions of 8-chloroguanosine **8** (1 mM) and *t*-BuOH (0.25 M) at pH ~7 are shown in Figure



1. The optical absorption spectrum taken 2 μs after the pulse (black squares) originated from the reaction of **8** with e<sub>aq</sub><sup>-</sup>. The disappearance of this species gave rise to a new transient species whose spectrum was taken 20 μs after the pulse (green triangles). By monitoring the reaction at 320 or 600 nm and analyzing the traces using the treatment for consecutive reactions, a first-order rate constant of (1.0 ± 0.3) × 10<sup>5</sup> s<sup>-1</sup> was obtained for the faster process relevant to the present study (insets of Figure 1). The last transient is identical to that obtained after the oxidation of **1a** by SO<sub>4</sub><sup>-</sup> at pH 7, i.e., radical **3** (Scheme 1). Similar results were obtained by replacing **8** with 8-iodoguanosine **9**. These findings are also very similar with previous data obtained from 8-bromoguanosine.<sup>14,15</sup>

Figure 2 shows the spectrum of the first observable species obtained 2 μs after the pulse for the three 8-halo derivatives, **6**, **8**, and **9**. The fact that 8-haloguanosines display the same optical spectrum suggests a common transient that has already lost the halogen atom. This species of uncertain structure decayed by first-order kinetics to produce the one-electron oxidized guanosine. As we will discuss later, this species was assigned to **7**, the tautomer of one-electron oxidized guanosine (see Scheme 1). It is worth also mentioning that we previously reported for bromide **6** the Arrhenius parameters log( $A/s^{-1}$ ) = 8.7 ± 0.4 and  $E_a$  = 23.0 ± 2.5 kJ mol<sup>-1</sup> for the observed decay,<sup>15</sup> a kinetic isotope effect  $k(\text{H}_2\text{O})/k(\text{D}_2\text{O})$  = 8.0 and a strong acceleration given by phosphate ( $k_{\text{phosp}} = 1.4 \times 10^8 \text{ M}^{-1} \text{ s}^{-1}$ ) and acids ( $k_{\text{H}^+} = 1 \times 10^{10} \text{ M}^{-1} \text{ s}^{-1}$ ).<sup>14</sup>

In order to test the behavior of the analogous 2'-deoxy-*ribo* nucleosides, we also considered 8-bromo-2'-deoxyguanosine (**13**). The spectral changes obtained from the pulse irradiation of a solution containing **13** at pH ~7 and **13** are reported in the Supporting Information. The results are very similar to those reported for the *ribo* derivative **6** (cf. Scheme 1). At pH 13, bromide **13** captures electrons and forms instantaneously a transient that is identical to that obtained after the oxidation of **1b** by Br<sub>2</sub><sup>•-</sup> at pH ~13, i.e., radical **4**. At pH 7, these experiments revealed again the formation of the two short-lived intermediates similar to those reported in Figure 1 for the 8-chloroguanosine. By monitoring the reaction at 600 nm and analyzing the trace using the treatment for consecutive reactions,

(24) A rate constant of 1.7 × 10<sup>10</sup> M<sup>-1</sup> s<sup>-1</sup> has been reported for the reaction of e<sub>aq</sub><sup>-</sup> with **1b**, using a photoionization method and single concentration experiment; see: Arce, R.; Rivera, J. J. *Photochem. Photobiol. A* **1989**, *49*, 219.

(25) Hansch, C.; Leo, A.; Taft, R. W. *Chem. Rev.* **1991**, *91*, 165.

(26) For the reactivity of aromatic compounds towards hydrated electrons and related Hammett correlations, see: Anbar, M.; Hart, E. J. *J. Am. Chem. Soc.* **1964**, *86*, 5633.

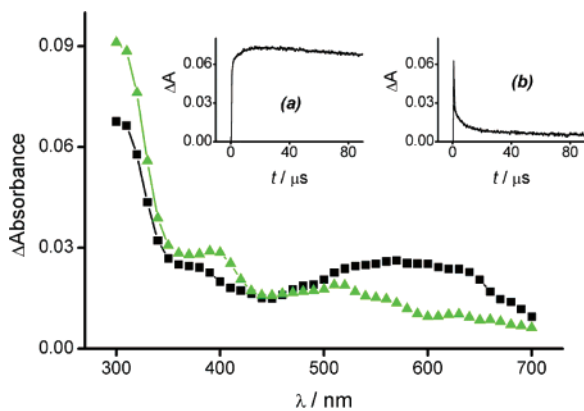


**Figure 1.** Absorption spectra obtained from the pulse radiolysis of Ar-purged solutions containing 1 mM **8** and 0.25 M *t*-BuOH at pH  $\sim$ 7 taken 2 (black square) and 20  $\mu$ s (green triangle) after the pulse; dose per pulse = 25 Gy, optical path = 2.0 cm. Insets: Time dependence of absorption at 320 (a) and 600 nm (b). The solid lines represent the fits to the data obtained using the treatment for consecutive reactions (see text). The initial fast decay in (b) is due to the disappearance of  $e_{aq}^-$ .

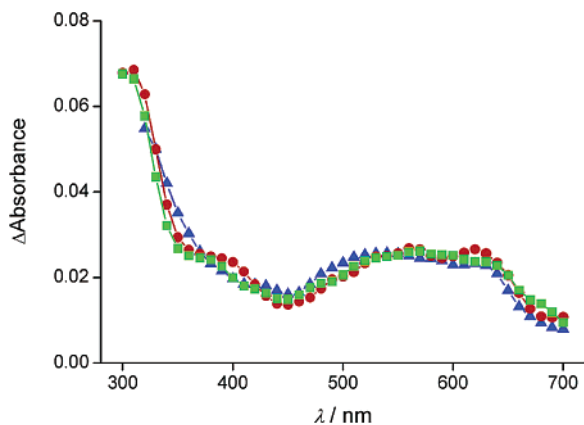


**Figure 2.** Absorption spectra obtained from the pulse radiolysis of Ar-purged solutions containing 1 mM **8** (green square), **6** (red circle), or **9** (blue triangle) and 0.25 M *t*-BuOH at pH  $\sim$ 7 taken 2  $\mu$ s after the pulse; optical path = 2.0 cm, dose per pulse = 25 Gy.

a first-order rate constant of  $1 \times 10^5 \text{ s}^{-1}$  was obtained. The last transient is very similar to that obtained after the oxidation of **1b** by  $\text{SO}_4^{\cdot-}$  at pH  $\sim$ 7, i.e., radical **3** (Scheme 1).

Next, we considered the 8-bromo derivatives **15–18** with partial or full alkylation at NH and/or  $\text{NH}_2$  moieties (Chart 1). Figure 3 shows the optical absorption spectra obtained from the reaction of a hydrated electron with **16** (red circle) and **17** (green triangle) in comparison with **6** (black square). The decay of these transients followed second-order kinetics, and their disappearance did not give other transients. Furthermore, these spectra are identical to that obtained after the oxidation of **21** and **22** by  $\text{SO}_4^{\cdot-}$  at pH  $\sim$ 7 (cf. Figure 4 of our preliminary communication for the couple **17**, **22**).<sup>15</sup> Very similar spectra having a sharp band around 350 nm and a broad band between 550 and 800 nm were also obtained from one-electron reduction of **18** and one-electron oxidation of **23**, indicating that the N=C double bond of the dimethylaminomethylene moiety does not play any special role. Figure 4 shows the optical absorption spectra obtained from the reaction of hydrated electrons with **15** (blue square) and the oxidation of **20** (red circle) by  $\text{Br}_2^{\cdot-}$ .<sup>1a</sup> The decay of these transients follows second-order kinetics, and their disappearance did not give other transients. It is gratifying to see the good superimposition and the band with  $\lambda_{\text{max}} = 610$

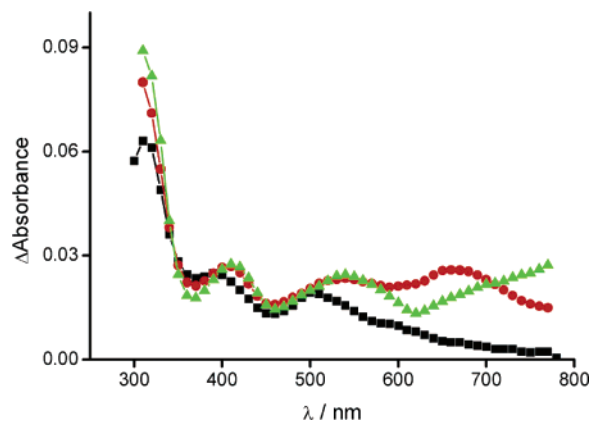


**Figure 3.** Absorption spectra obtained from the pulse radiolysis of Ar-purged solutions at pH  $\sim$ 7 containing 1 mM **6** (black square), **16** (red circle), or **17** (green triangle) and 0.25 M *t*-BuOH taken 2 (red circle, green triangle) or 40  $\mu$ s (black square) after the pulse; optical path = 2.0 cm, dose per pulse = 24 Gy.

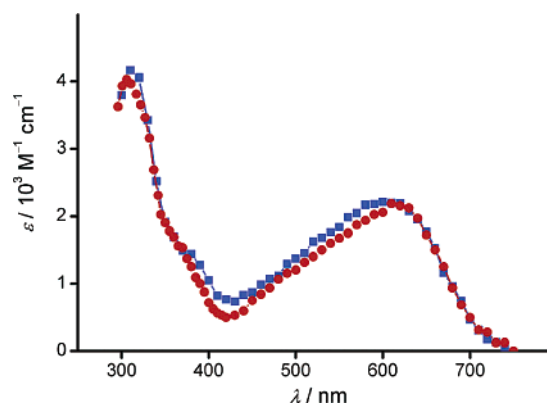
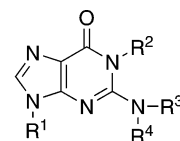


**Figure 4.** Absorption spectrum (blue square) obtained from the pulse radiolysis of Ar-purged solutions containing 0.5 mM **15** at pH  $\sim$ 7 with 0.25 M *t*-BuOH, taken 10  $\mu$ s after the pulse; optical path = 2.0 cm, dose per pulse = 24 Gy. Absorption spectrum (red circle) taken from ref 1a and refers to the reaction of  $\text{Br}_2^{\cdot-}$  with **20**.

nm. Therefore, the same species were obtained from the reaction of the hydrated electron with 8-bromo derivatives **15–18** and from the oxidation of guanosines **20–23**.



**20:**  $\text{R}^1 = \text{ribose}$ ,  $\text{R}^2 = \text{Me}$ ,  $\text{R}^3 = \text{R}^4 = \text{H}$

**21:**  $\text{R}^1 = \text{ribose}$ ,  $\text{R}^2 = \text{H}$ ,  $\text{R}^3 = \text{Et}$ ,  $\text{R}^4 = \text{H}$

**22:**  $\text{R}^1 = \text{ribose}$ ,  $\text{R}^2 = \text{H}$ ,  $\text{R}^3 = \text{R}^4 = \text{Et}$

**23:**  $\text{R}^1 = \text{dR}$ ,  $\text{R}^2 = \text{H}$ ,  $\text{R}^3 \text{R}^4 = \text{NCHNMe}_2$

$\gamma$ -Radiolysis and products studies of 8-halo substituted guanine derivatives have also been carried out in a similar manner as described for **6**.<sup>14</sup> Deaerated aqueous solutions containing **8** or **9** (ca. 1.5 mM) and *t*-BuOH (0.25 M) at pH  $\sim$ 7 were irradiated under stationary-state conditions with a dose rate of ca. 20 Gy/min followed by HPLC analysis. Compound **1a** was the only detectable product, and mass balances were close to 100%. Analysis of the data in terms of radiation chemical yield ( $G$ )<sup>27</sup> gives  $G(-\mathbf{8}) = 0.35$  and  $G(\mathbf{1a}) = 0.32 \mu\text{mol J}^{-1}$  for chloride **8** and  $G(-\mathbf{9}) = 0.34$  and  $G(\mathbf{1a}) = 0.31 \mu\text{mol J}^{-1}$  for iodide **9**. Analogously, deaerated aqueous solutions

containing **13**, **15**, **16**, or **17** (ca. 1.5 mM) and *t*-BuOH (0.25 M) at pH  $\sim$ 7 were irradiated under stationary-state conditions with a dose rate of ca. 15 Gy min<sup>-1</sup> followed by HPLC analysis.<sup>28</sup> Compounds **1b**, **20**, **21**, and **22** were the only detectable products, and mass balances were close to 100%. Analysis of the data in terms of radiation chemical yield (*G*) gives  $G(-\mathbf{13}) = 0.34$ ,  $G(\mathbf{1b}) = 0.31$ ,  $G(-\mathbf{15}) = 0.36$ ,  $G(\mathbf{20}) = 0.31$ ,  $G(-\mathbf{16}) = G(\mathbf{21}) = 0.33$ , and  $G(-\mathbf{17}) = 0.34$ ,  $G(\mathbf{22}) = 0.30 \mu\text{mol J}^{-1}$  (see Supporting Information). Taking into account that  $G(e_{\text{aq}}^-) + G(\text{H}^\bullet) = 0.33 \mu\text{mol J}^{-1}$ , our results lead to the conclusion that solvated electrons and hydrogen atoms react with 8-haloguanine derivatives to yield quantitatively the dehalogenated nucleosides. These results are very similar to those reported for bromide **6**.<sup>14</sup> In D<sub>2</sub>O the quantitative incorporation of deuterium at the 8-position was also observed for bromide **6**, indicating that the hydrogen in the 8-position originates from water.<sup>14</sup>

**Fate of Electron Adducts of Other Derivatives.** Pulse radiolysis studies of the reaction of  $e_{\text{aq}}^-$  with some derivatives that have 8-substituents other than halogen atoms have also been considered. In particular, compounds **10**, **11**, **12**, and **14** have been tested and found to behave differently from the analogous 8-halo derivatives. Indeed, the one-electron oxidized guanine derivative **3** is not an intermediate in the reaction path. A detailed study of these derivatives is in progress.

**DFT Calculations.** Using DFT calculations at the B3LYP/6-31G\* level, we showed that the radical anion of 8-bromo-2'-deoxyadenosine is not stable and loses Br<sup>-</sup> to form the neutral  $\sigma$ -type radical at C8.<sup>29a</sup> In accord with experiments<sup>29,30</sup> this radical was computed to undergo radical translocation from C8 to C5' and subsequent 6-exo-trig radical cyclization with relatively low activation barriers to afford the 5',8-cyclonucleoside. In the present study B1B95/6-31+( $\lambda=0.7$ )G\*\* calculations show that the radical anion of 8-bromo-2'-deoxyadenosine remains unstable while the radical anion of 8-bromo-2'-deoxyguanosine (**24**) is stable. This different behavior can be rationalized considering the electron distribution in the SOMO of the radical anions computed at the geometry of the neutral molecule. We showed that in the frozen radical anion of 8-bromo-2'-deoxyadenosine the unpaired electron is substantially localized at C8.<sup>29a</sup> However, the unpaired electron tends to occupy the antibonding  $\sigma^*_{\text{C8-Br}}$  MO upon relaxing the structural parameters favoring the loss of Br<sup>-</sup>. In the case of **24**, the electronic distribution in the SOMO of the radical anion (Figure 5) shows that the unpaired electron is localized on the six-membered ring mainly at the C2 carbon atom that is surrounded by electronegative nitrogen atoms. In particular, the electron density in the SOMO of the frozen radical anion **24** is 0.06 at C8, 0.01 at Br, and 0.36 at C2-NH<sub>2</sub>, whereas in the frozen radical anion of 8-bromo-2'-deoxyadenosine it is 0.22 at C8, 0.04 at Br, and 0.19 at C2. Thus, the radical anion **24** does not directly lose Br<sup>-</sup> upon relaxing the structural parameters since the electron density in the SOMO at C8 is small.

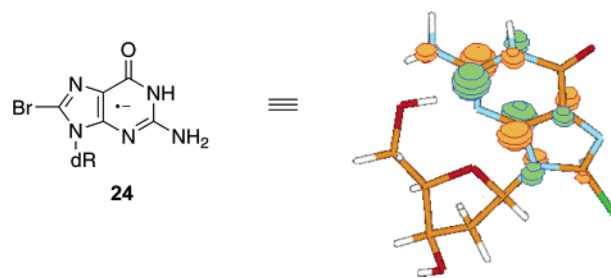


**Figure 5.** SOMO of radical anion **24** computed at the geometry of a neutral molecule at the B1B95/6-31+( $\lambda=0.7$ )G\*\* level.

	$\lambda$	<i>f</i>
<b>24</b>	324	0.076
	336	0.014
	402	0.014
	460	0.018
	510	0.057
<b>25</b>	311	0.020
	345	0.015
	363	0.105
	423	0.036
<b>3 (R=2-deoxyribose)</b>	280	0.057
	347	0.040
	378	0.014
	510	0.012

**Figure 6.** TD-B3LYP/6-311G\*\* optical transitions (wavelength  $\lambda$  and oscillator strength *f*) for radicals **24**, **25**, and **3**.

Time-dependent DFT (TD-B3LYP/6-311G\*\*) calculations were carried out to characterize the first observable species that has a characteristic absorbance around 600 nm in a neutral solution since this theoretical method was previously found by us to provide reliable optical transitions in nucleosides.<sup>29a,31</sup> Figure 6 shows that the radical anion **24** is predicted to have no optical absorption above 510 nm. In a neutral solution the initial electron adduct should be rapidly protonated, and therefore, calculations were carried out on the radical anion protonated at N7 (**25**) as suggested previously.<sup>14</sup> No optical transition with appreciable oscillator strength *f* is computed at wavelengths longer than 425 nm in evident contrast with the experimental spectrum displayed in Figure 1 detected 2  $\mu$ s after the pulse. On the other hand, Figure 6 shows that the optical transitions computed for **3** ( $\lambda_{\text{max}} = 280$  with a shoulder at 347 nm and a weak band at 510 nm) are in good accord with those assigned with certainty to this radical ( $\lambda_{\text{max}} = 310$  nm with a shoulder at 380 nm and a weak band at 500 nm).

Next, TD-DFT calculations were carried out on the 8-bromo-9-methylguanine radical anion (**26**) protonated at any other possible sites, since preliminary calculations showed that the computed optical spectra described above do not change significantly replacing the sugar moiety with a methyl group.<sup>32</sup> No optical transition is predicted to occur at wavelengths longer than 500 nm (see Supporting Information). Interestingly, the

(27) The disappearance of the starting material or the appearance of the product (mol/kg) divided by the absorbed dose (1 Gy = 1 J/kg) gives the radiation chemical yield, i.e.,  $G(-\mathbf{8})$  or  $G(\mathbf{1a})$ , respectively.

(28) The solution at pH  $\sim$ 7 (i.e., natural without additives) before and after the irradiation dose of 2 kGy gave pH 7.6 and 5.7, respectively.

(29) (a) Chatgililoglu, C.; Guerra, M.; Mulazzani, Q. G. *J. Am. Chem. Soc.* **2003**, *125*, 3839. (b) Flyunt, R.; Bazzanini, R.; Chatgililoglu, C.; Mulazzani, Q. G. *J. Am. Chem. Soc.* **2000**, *122*, 4225.

(30) Jimenez, L. B.; Encinas, S.; Miranda, M. A.; Navacchia, M. L.; Chatgililoglu, C. *Photochem. Photobiol. Sci.* **2004**, *3*, 1042.

(31) Chatgililoglu, C.; Ferreri, C.; Bazzanini, R.; Guerra, M.; Choi, S.-Y.; Emanuel, C. J.; Horner, J. H.; Newcomb, M. *J. Am. Chem. Soc.* **2000**, *122*, 9525.

(32) Compare transitions reported in Figures 6 and 8, and Tables S1 and S2.

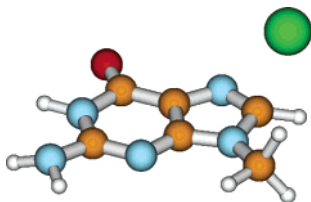
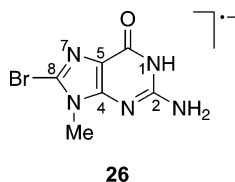
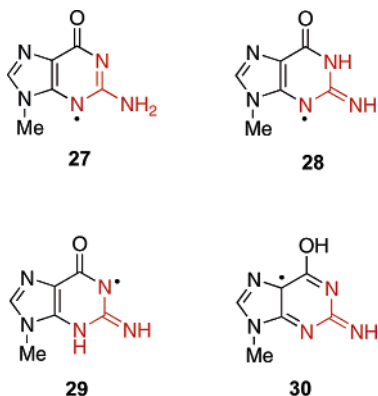


**Figure 7.** Structure of the 8-bromo-9-methylguanine radical anion protonated at C8 at the B1B95/6-31+G\*\* level.

radical protonated at N7 is more stable among the heteroatom protonated radicals. However, the energy barrier (181.6 kJ mol<sup>-1</sup> at the B1B95/6-31+G\*\* level) for the intramolecular proton transfer from N7 to C8 is computed to be much higher than that of 23.0 kJ mol<sup>-1</sup> observed experimentally.



Enlarging the basis set does not change significantly the energy barrier (180.7 kJ mol<sup>-1</sup> at the B1B95/6-311++G(3df,-2p)//B1B95/6-31+G\*\* level), while inclusion of the effect of a polarizable continuum model for the aqueous solution with the PCM method increases slightly the energy barrier (192.5 kJ mol<sup>-1</sup> at the PCM/B1B95/6-31+G\*\*//B1B95/6-31+G\*\* level). On the other hand, protonation at C8 does not produce a “normal” protonated form of the 8-bromo-9-methylguanine radical. The C8–Br bond length largely increases with respect to the normal C–Br bond length, and a loose  $\pi$ -complex is formed, where the Br atom is placed above the molecular plane at a distance of 2.33 Å (see Figure 7). This complex is more stable than the N7-protonated form by 42.0 kJ mol<sup>-1</sup>, so it is likely that an initial protonation occurs easier at C8 rather than at N7. The loose  $\pi$ -complex is prompt to lose Br<sup>-</sup>, so these theoretical findings suggest that the first observable species in the pulse radiolysis had already lost Br<sup>-</sup> and could be a tautomer of guanyl radical **3**. The optical transitions of the one-electron oxidized 9-methylguanine (**27**) and its tautomers bearing an iminic group at C2 (**28**, **29**, and **30**) are reported in the Supporting Information. Interestingly, a weak band at wavelengths in the range 550–650 nm is computed only for the tautomer **28**.



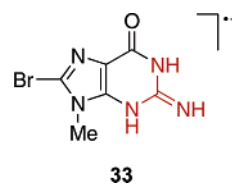
Similar results are obtained by replacing the Me group at position 9 with 2-deoxyribose (see **7** in Figure 8). The optical

	$\lambda$	$f$
<b>7</b> (R=2-deoxyribose)	283	0.056
	345	0.026
	379	0.013
	620	0.047
<b>31</b>	282	0.058
	383	0.032
	660	0.037
<b>32</b>	280	0.140
	398	0.063
	493	0.014
	1035	0.016

**Figure 8.** TD-B3LYP/6-311G\*\* optical transitions (wavelength  $\lambda$  and oscillator strength  $f$ ) for radicals **7**, **31**, and **32**.

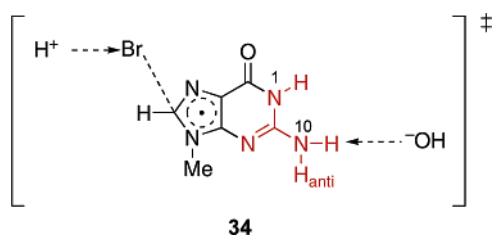
transitions computed for this tautomer are in good accord with the absorption spectrum of the first observable species displayed in Figure 1 or 2. TD-DFT calculations were performed also on radicals **31** and **32** to confirm the assignments discussed above, i.e., obtained either from the reduction of **15** and **17** or by oxidation of **20** and **22**. The first radical has surely an iminic structure at C2, whereas the second one is surely deprotonated at N1. Figure 8 shows that an optical transition with appreciable oscillator strength is computed above 600 nm for radical **31** as expected for the iminic substitution at C2. The computed optical transitions ( $\lambda_{\max} = 282$  with a shoulder at 383 nm and a band at 660 nm) are in good accord with the experimental spectrum reported in Figure 4. The agreement between theory and experiments is good also for the absorption spectrum of radical **32**.<sup>33</sup>

Initial deprotonation at N10 could result from N10–H to N3–H tautomerization during formation of the radical anion. However, B1B95/6-31+( $\lambda=0.7$ )G\*\* calculations performed on the radical anion **26** and on its tautomer **33** show that **26** is much more stable than **33** by 58.2 kJ mol<sup>-1</sup>. This result was confirmed by high-level ab initio calculations, the energy difference being 54.4 kJ mol<sup>-1</sup> at the QCISD/6-31+( $\lambda=0.7$ )-G\*\*//B1B95/6-31+( $\lambda=0.7$ )G\*\* level.



Alternatively, initial deprotonation at N10 by means of HO<sup>-</sup> could occur during elimination of Br<sup>-</sup> from the  $\pi$ -complex as HBr. Indeed, B1B95/6-31+G\*\* calculations show that the transition state **34** for elimination of H10(syn) is much more stable than the transition states for elimination of H1 by 14.1 kJ mol<sup>-1</sup> and of H10(anti) by 18.0 kJ mol<sup>-1</sup>.

(33) Substitution of the hydrogen of the aminic group at N10 produces in the experimental spectrum the appearance of a new weak band above 800 nm (Figure 6) that is computed to occur at about 1000 nm at the TD-B3LYP/6-311G\*\*//B1B95/6-31+G\*\* level.



Analogous assignments for the structure **7** have been reported analyzing the ESR/ENDOR spectra of the decay product of the guanine radical cations in single crystals of 2'-deoxyguanosine 5'-monophosphate<sup>11</sup> and 3',5'-cyclic guanosine monophosphate.<sup>12</sup> Two proton hyperfine splittings (hfs) of  $-5.0$  and  $-9.5$  G were determined and assigned to the  $\alpha$ -proton bonded to C8 and to N10, respectively, on the base of the  $\pi$ -spin density distribution calculated with the INDO RHF-CI method. B3LYP/6-311G\*\*//B1B95/6-31+G\*\* calculations were carried out on the 2'-deoxyguanosine radical cation deprotonated at N1 (**3**) and N10 (**7**). The hfs couplings computed for **3** ( $a_{\text{H8}} = -7.5$  G,  $a_{\text{H10}} = -1.2$  and  $-1.7$  G) are in disaccord with the experimental values, while those computed for **7** ( $a_{\text{H1}} = -0.6$  G,  $a_{\text{H8}} = -6.1$  G,  $a_{\text{H10}} = -8.6$  G) are in good accord with experiment.<sup>11</sup> This firmly supports the formation of the N10 deprotonated guanine radical cation in the solid state.

The distribution of the unpaired electron in the SOMO of the 2'-deoxyguanosine radical cation deprotonated at N1 (**3**) and at N10 (**7**) is shown in Figure 9.

In the aminic form the unpaired electron is mainly localized at the N3, O6, C5, and C8 atoms. This is confirmed from the computed spin density reported in Table 2. Hence, the radical can be represented by the resonance structures A(I), A(II), A(III), A(IV), and A(V) shown in Scheme 2. However, structure A(V) gives a negligible contribution to the SOMO. This suggests that the resonance charged structure A(VI) bearing a negative charge at N1 and a positive charge at N10 is more important than structure A(V).

In the iminic forms the spin density at C5, C8, and N3 does not change significantly, and the radical can be represented by the resonance structures B(I), B(II), B(III), B(IV), and B(V) shown in Scheme 3. As expected a large spin density is localized at N10. Surprisingly, the spin density is small at O6, B(I). This is due to the prevalence, in this case, of a charged amidic structure B(VI) over the resonance structure B(I).

The importance of the ionic structures A(VI) and B(VI) is supported by the variation of the atomic charges at the guanosine atoms (see Table 2). The importance of A(VI) is evidenced by the increase of the positive charge at N10 on going from the iminic to the aminic form, while the importance of B(VI) is evidenced by the increase of the negative charge at N1 on going from the iminic to the aminic form. Interestingly, the ionic structures A(VI) and B(VI) are expected to favor the tautomerizations between N1 and N10.

Our preliminary calculations at the B3LYP/6-31G\* level showed that the reaction barrier for the direct tautomerization from **7** to **3** is large ( $183.7$  kJ mol<sup>-1</sup> without ZPVE) in evident contrast with the activation energy measured for this tautomerization ( $23.0$  kJ mol<sup>-1</sup>).<sup>15</sup> However, in analogy with the keto-enol tautomerization in guanine<sup>34</sup> and 8-oxo-7,8-dihydro-

**Table 2.** Spin Density ( $\rho$ ) and Atomic Charges ( $q$ ) at the Guanosine Atoms in the Aminic and Iminic Form of the Deprotonated One-Electron Oxidized 2'-Deoxyguanosine Computed at the B3LYP/6-311G\*\*//B1B95/6-31+G\*\* Level

atom	aminic		iminic	
	$\rho$	$q^a$	$\rho$	$q^a$
N1	0.01	-0.38	0.01	-0.18
C2	-0.02	0.43	-0.12	0.40
N3	0.30	-0.42	0.34	-0.40
C4	-0.01	0.43	-0.05	0.40
C5	0.34	-0.09	0.29	-0.09
C6	-0.08	0.36	-0.03	0.44
O	0.21	-0.29	0.03	-0.32
N7	-0.05	-0.27	-0.03	-0.28
C8	0.27	0.34	0.22	0.34
N9	-0.02	-0.40	-0.01	-0.39
N10	0.06	0.04	0.39	-0.17

<sup>a</sup> Mulliken atomic charges with hydrogen summed into heavy atoms.

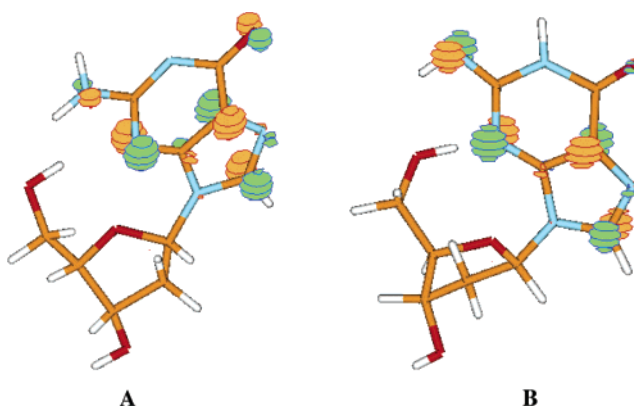


**Figure 9.** SOMO of the aminic (A) and iminic (B) forms of the deprotonated one-electron oxidized 2'-deoxyguanosine computed at the B3LYP/6-311G\*\* level.

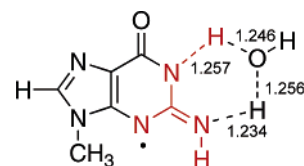


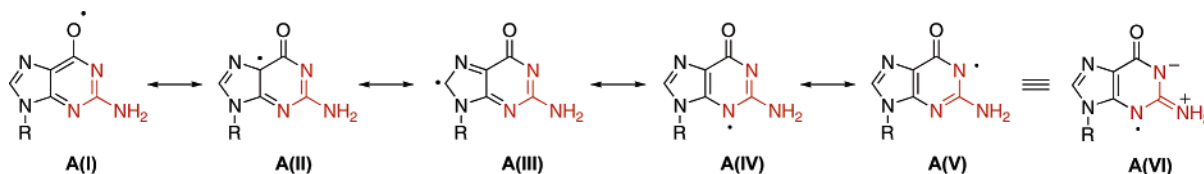
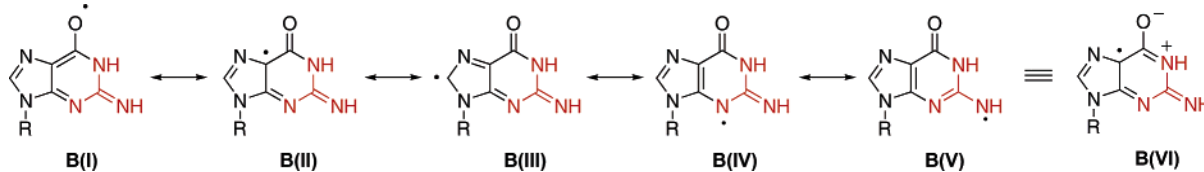
**Figure 10.** Structure of the transition state for the water-assisted tautomerization **28**→**27** computed at the B1B95/6-311G\*\* level. Distances are in Å.

guanine,<sup>35</sup> the water-assisted proton transfer was computed to occur with a much lower reaction barrier ( $18.8$  kJ mol<sup>-1</sup>). B1B95/6-31+G\*\* calculations with a ZPVE correction show a similar trend. The reaction barrier is computed to be large in the gas phase ( $172.0$  kJ mol<sup>-1</sup>). Neither enlarging the basis set nor inclusion of the effect of a polarizable continuum model for the aqueous solution significantly changes the energy barrier ( $169.9$  kJ mol<sup>-1</sup> at the B1B95/6-311++G(3df,2p)//B1B95/6-31+G\*\* level and  $172.4$  kJ/mol at the PCM/B1B95/6-31+C\*\*//B1B95/6-31+G\*\* level). On the other hand, the water assisted proton transfer is computed to be  $21.3$  kJ mol<sup>-1</sup> at the PCM/B1B95/6-31+G\*\*//B1B95/6-31+G\*\* level in good accord with experiment (Figure 10).

DFT calculations were also performed on 8-substituted 9-methylguanines to compare their vertical electron affinities (VEA) with the rate constants for the reaction of  $e_{\text{aq}}^-$  with

(34) Gorb, L.; Leszczynski, J. *J. Am. Chem. Soc.* **1998**, *120*, 5024.

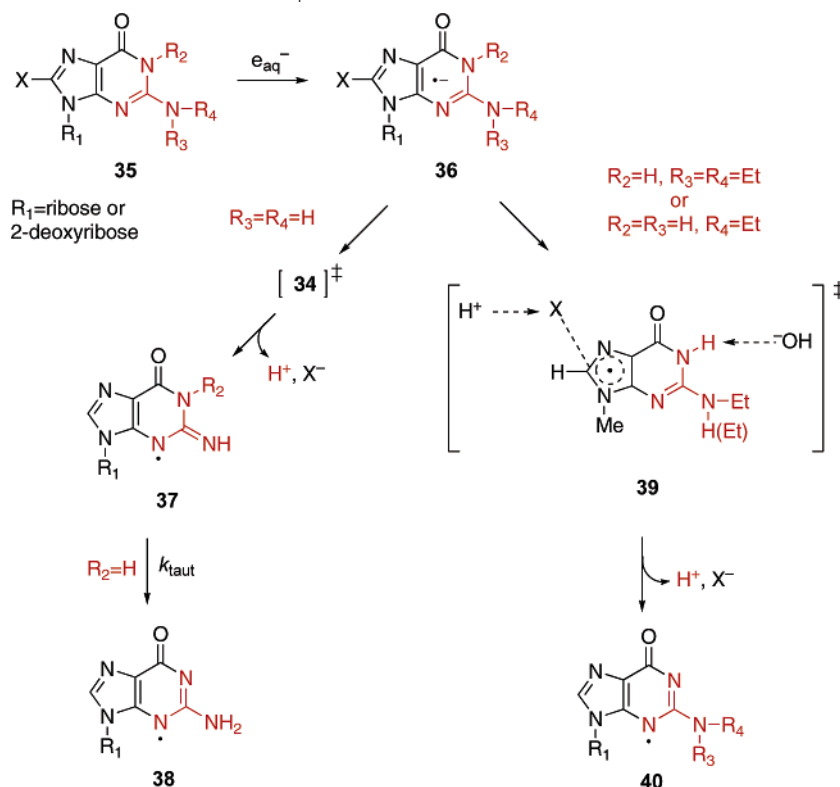
(35) Llano, J.; Eriksson, L. A. *Phys. Chem. Chem. Phys.* **2004**, *6*, 4707.

**Scheme 2.** Possible Resonance Structures for Radical **3** (cf. Figure 9A)**Scheme 3.** Possible Resonance Structures for Radical **7** (cf. Figure 9B)

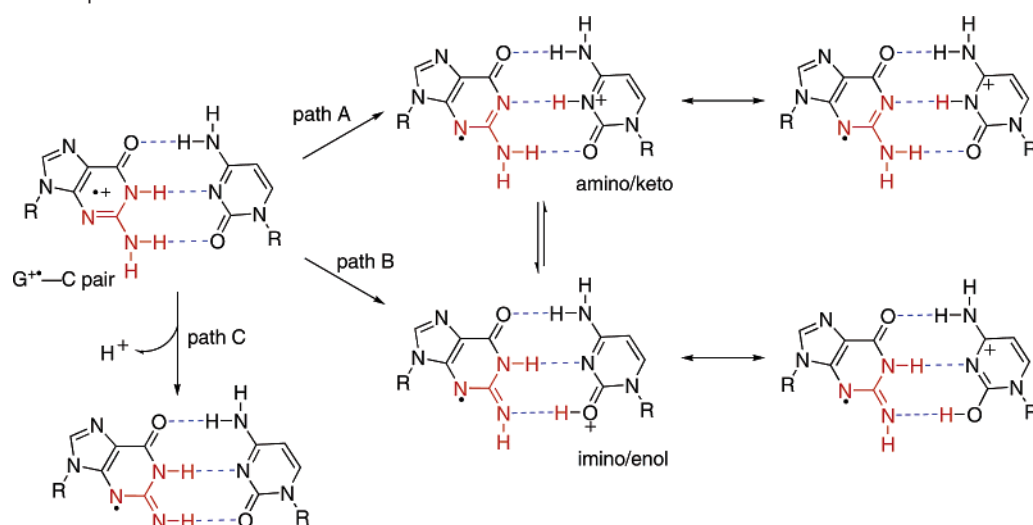
8-substituted guanosines (Table 1). At the B1B95/6-31+-( $\lambda=0.7$ )G\*\* level, the following (VEA/eV) values were obtained: H(-1.47), Cl(-1.23), Br(-1.20), HO(-1.48), MeS(-1.45), N<sub>3</sub>(-0.56), NH<sub>2</sub>NH(-1.51).<sup>36</sup> By comparison, the rate constants can be predicted only qualitatively. The substitution of H with a strong electron acceptor such as N<sub>3</sub> increases considerably the vertical electron affinities by about 1 eV. This is in accord with the large increase of the rate constant for the reaction with e<sub>aq</sub><sup>-</sup>. Halogen substitution moderately stabilized the “frozen” radical anion. This is in accord with an intermediate increase of the rate constants for Cl and Br derivatives. However, there is disagreement between Cl and Br derivatives. In accord with experiment the donor groups MeS, HO, and NH<sub>2</sub>NH do not substantially affect the stability of the radical anion.

**Reaction Mechanism.** On the basis of the experimental findings and the attribution of the optical absorption transition by TD-DFT calculations, we propose the mechanism illustrated in Scheme 4 for the reaction of e<sub>aq</sub><sup>-</sup> with 8-halo substituted

guanine derivatives **35**. The pristine electron adduct **36** is not observed because it is rapidly protonated ( $k > 5 \times 10^6 \text{ s}^{-1}$ ) at the C8 position to give Br<sup>-</sup> and the one-electron oxidized guanine derivative **37** or **40** depending on the substituents at the N1 and N10 positions. In the case of unsubstituted derivatives at positions N1 and N10 (e.g., **6**, **8**, **9**, and **13**), the first observable transient species is **37**. The subsequent tautomerization **37**→**38** occurs with an activation energy of 23 kJ mol<sup>-1</sup> ( $k_{\text{taut}} = 1 \times 10^5 \text{ s}^{-1}$  at 22 °C) through a complex transition state involving a water molecule (Figure 10). The large kinetic isotope effect and the strong acceleration given by phosphate and acids are also in favor of the tautomerization. For R<sub>2</sub> = Me, radical **37** is blocked in the iminic form and therefore no tautomerization is observed. On the other hand, the protonation of pristine electron adduct **36** affords Br<sup>-</sup> and **40** when single or double alkyl substitution at N10 is present. The mechanism proposed above for deprotonation (see **34**) could also explain why deprotonation at N10 does not occur in the former case

**Scheme 4.** Proposed Mechanism for the Reaction of e<sub>aq</sub><sup>-</sup> with 8-Halo Substituted Guanine Derivatives **35**



**Scheme 5.** Possible Deprotonation Paths of G<sup>+</sup>–C Pair<sup>a</sup>

<sup>a</sup> For clarity of keto/enol tautomerization, the resonance forms of C(+H<sup>+</sup>) are given.

(R<sub>3</sub> = H, R<sub>4</sub> = Et). B1B95/6-31+G\*\* calculations show that **16** adopts a conformation with H10 anti with respect to N1, the syn conformation lying 5.3 kJ mol<sup>-1</sup> higher in energy. Thus deprotonation in the  $\pi$ -complex **39** should be easier at N1 than at N10.

## Conclusions

Previously, the absorption spectra of tautomer **3** were obtained by one-electron oxidation of **1a** or **1b** at a natural pH value,<sup>1,2</sup> whereas the EPR/ENDOR spectra of tautomer **7** resulted upon X-irradiation of 2'-deoxyguanosine 5'-monophosphate in the solid state at 10 K.<sup>11</sup> However, no evidence of any direct connection between the two tautomers was provided. Our work here demonstrates the first directly observed differences of the two tautomeric forms of one-electron oxidized guanosine or 2'-deoxyguanosine. Using the reaction of hydrated electrons (e<sub>aq</sub><sup>-</sup>) with 8-haloguanosine or 8-halo-2'-deoxyguanosine, the observed two short-lived intermediates were assigned to tautomers **37** and **38**. Initially, the less stable form (**37**) is obtained from the protonation of 8-haloguanine electron adduct, and its water-assisted tautomerization to **38** has an activation energy of 23 kJ mol<sup>-1</sup>.

Our findings raise an intriguing possibility when extended to the deprotonation behavior of guanine radical cations in DNA. Since guanine moieties have the lowest oxidation potential within the four DNA bases, the hole migrates to G–C pairs.<sup>37</sup> It has been suggested that the corresponding G<sup>+</sup>–C pair undergoes a facile proton shift along its central hydrogen bond (Scheme 5, path A).<sup>38</sup> The alternative paths B and C have

received little or no attention.<sup>39</sup> Kobayashi and Tagawa investigated the oxidation of double-stranded oligonucleotides containing G–C moieties by pulse radiolysis.<sup>6</sup> Interestingly, they found two short-lived intermediates, and their absorption spectra strongly resemble those in Figure 1 but with an opposite time sequence. The growth observed at 625 nm fits well with a biexponential curve with rate constants of  $\sim 1.3 \times 10^7$  and  $\sim 3.0 \times 10^6$  s<sup>-1</sup>. The two steps tentatively were assigned to the deprotonation of the N1 proton of G in DNA (path A) and subsequent deprotonation of C(+H<sup>+</sup>) by a water molecule. The present work suggests an alternative scenario, where the second observed transient may be due to the iminic form of the guanine radical. Consequently, the two consecutive reactions become the proton shift along its central hydrogen bond (path A) followed by a “tandem tautomerization” from the amino/keto to imino/enol structures. Zewail and co-workers in DNA models have observed this type of tautomerization.<sup>40</sup> Further experimental and theoretical studies are required in order to understand the details of the tautomerization of the one-electron oxidized G–C pair in DNA. The fact that reduction of 8-bromo-2'-deoxyguanosine incorporated in single- or double-stranded oligonucleotides and G-quadruplex behave similar to simple nucleosides<sup>16,18,19</sup> points out the need of a thorough study of the transient species in these reactions. In this area, we are currently examining these and other systems.

## Experimental Section

**Materials.** Compounds **13**, **14**, and **18** were commercially available from Berry & Associates (Ann Arbor, MI). Compounds **1a**, **1b**, and *t*-BuOH were purchased from Sigma-Aldrich or Fluka. Potassium peroxydisulfate and phosphate buffer were purchased from Merck. Acetonitrile and methanol, both HPLC grade, were from Scharlau. Water was purified through a Millipore (Milli-Q) system. Compounds **8**,<sup>41</sup> **9**,<sup>42</sup> **10**,<sup>43</sup> **11**,<sup>44</sup> **12**,<sup>44</sup> **15**,<sup>45</sup> **16**,<sup>46</sup> **17**,<sup>46</sup> **20**,<sup>45</sup> **21**,<sup>46</sup> and **22**<sup>46</sup> were prepared following known procedures.

**Pulse Radiolysis.** Pulse radiolysis with optical absorption detection was performed by using the 12 MeV linear accelerator, which delivered

(36) The corresponding energies of the lowest unoccupied MO ( $E_{LUMO}/\text{eV}$ ) are H(-0.09), Cl(-0.29), Br(-0.30), HO(-0.08), MeS(-0.04), N<sub>3</sub>(-1.16), NH<sub>2</sub>NH(-0.02).

(37) For some reviews on hole migration through the stacked bases of duplex DNA, see: (a) Holmlin, R. E.; Dandliker, P. J.; Barton, J. K. *Angew. Chem., Int. Ed.* **1997**, *36*, 2714. (b) Kelley, S. O.; Barton, J. K. *Science* **1999**, *283*, 375. (c) Grinstaff, M. W. *Angew. Chem., Int. Ed.* **1999**, *38*, 3629. (d) Giese, B. *Acc. Chem. Res.* **2000**, *33*, 631. (e) Schuster, G. B. *Acc. Chem. Res.* **2000**, *33*, 253. (f) Lewis, F. D.; Lestingner, R. L.; Wasielewski, M. R. *Acc. Chem. Res.* **2001**, *34*, 159. (g) Giese, B. *Annu. Rev. Biochem.* **2002**, *71*, 51.

(38) (a) Steenken, S. *Chem. Rev.* **1989**, *89*, 503. (b) Steenken, S. *Biol. Chem.* **1997**, *378*, 1293. (c) Li, X.; Cai, Z.; Sevilla, M. D. *J. Phys. Chem. B* **2001**, *105*, 10115. (d) Weatherly, S. C.; Yang, I. V.; Thorp, H. H. *J. Am. Chem. Soc.* **2001**, *123*, 1236.

(39) Reynisson, J.; Steenken, S. *Phys. Chem. Chem. Phys.* **2002**, *4*, 5346.

(40) (a) Douhal, A.; Kim, S. K.; Zewail, A. H. *Nature* **1995**, *378*, 260. (b) Zewail, A. H. *J. Phys. Chem.* **1996**, *100*, 12701.

(41) Ryu, E. K.; MacCoss, M. J. *Org. Chem.* **1981**, *46*, 2819.

(42) Lipkin, D.; Howard, F. B.; Nowotny, D.; Sano, M. *J. Biol. Chem.* **1963**, *238*, 2249.

20–200 ns electron pulses with doses between 5 and 50 Gy, by which HO•, H•, and e<sub>aq</sub><sup>-</sup> are generated with 1–20 μM concentrations. The pulse irradiations were performed at room temperature (22 ± 2 °C) on samples contained in Spectrosil quartz cells of a 2 cm optical path length. Solutions were protected from the analyzing light by means of a shutter and appropriate cutoff filters. The bandwidth used throughout the pulse radiolysis experiments was 5 nm. The radiation dose per pulse was monitored by means of a charge collector placed behind the irradiation cell and calibrated with a N<sub>2</sub>O-saturated solution containing 0.1 M HCO<sub>2</sub><sup>-</sup> and 0.5 mM methyl viologen, using  $G\epsilon = 9.66 \times 10^{-4} \text{ m}^2 \text{ J}^{-1}$  at 602 nm for the monitored reduced form of methylviologen, MV<sup>+</sup>.<sup>47a</sup>  $G(X)$  represents the number of moles of species X formed, consumed, or altered per joule of energy absorbed by the system.

**Continuous Radiolysis and Product Analysis.** Continuous radiolysis were performed at room temperature (22 ± 2 °C) on 4–200 mL samples using a <sup>60</sup>Co-Gammacell, with dose rates of 12–20 Gy min<sup>-1</sup>. The absorbed radiation dose was determined with the Fricke chemical dosimeter, by taking  $G(\text{Fe}^{3+}) = 1.61 \mu\text{mol J}^{-1}$ .<sup>47b</sup> The reactions of 8-bromosubstituted derivatives with e<sub>aq</sub><sup>-</sup> were investigated using de-aerated aqueous solutions containing 1.5 mM substrate and 0.25 M *t*-BuOH at pH ~7. A solution of 210 mL was irradiated with a total dose up to 2 kGy and monitored by HPLC. Products were identified and quantified by comparison with authentic samples. Reversed-phase HPLC analysis was performed on a Waters apparatus equipped with an analytical column (Waters XTERRA, 150 × 4.6 mm, 5 μm), a Waters 2996 photodiode array detector at a fixed wavelength of 254 nm, and a Waters 600 controller. The chromatographic system used for analytical experiments consisted of acetonitrile and water as eluents (linear gradient from 0 to 20% of acetonitrile over 25 min) at a flow rate of 1 mL min<sup>-1</sup>.

**Computational Details.** Hybrid meta DFT calculations with the B1B95 (Becke88<sup>48</sup>–Becke95<sup>49</sup> one-parameter model for thermochemistry) functional<sup>50</sup> were carried out using the Gaussian 03 system of programs.<sup>51</sup> This HMDFT model was found to give excellent performance for thermochemistry<sup>50,52,53</sup> and molecular geometries<sup>52,53</sup> as well as for electron affinities.<sup>53</sup> An unrestricted wavefunction was used for radical species. Optimized geometries and total energies were obtained employing the valence double- $\zeta$  basis set supplemented with polarization functions and augmented with diffuse functions on heavy atoms.

However, the use of standard diffuse functions in this basis set (6-31+G\*\*) gives an unreliable description of the radical anion of **13** as expected for molecules having negative gas-phase vertical electron affinities.<sup>54a</sup> For example the extra electron in the radical anion of **13** is localized at the *s* diffuse atomic orbitals of the carbon atoms (mainly at C2). The use of moderate diffuse functions with a scaling factor  $\lambda$  of 0.7 provides reliable results according to the criteria outlined in ref 54b. Hence the B1B95 calculations for **13** and 8-bromo-2'-deoxyadenosine and for their radical anions were carried out using the 6-31+( $\lambda=0.7$ )G\*\* basis set. Moderate diffuse functions were also used to estimate the vertical electron affinity (VEA) of 8X-9-methylguanines (X = H, Cl, Br, OH, SMe, N<sub>3</sub>, NHHN<sub>2</sub>). The energy barriers for H transfer from N7 to C8 in the radical anion of 8-bromo-9-methylguanine protonated at N7 and for tautomerization from the imino to amino form of the deprotonated one-electron oxidized 9-methylguanine were corrected for the zero-point vibrational energy (ZPVE) computed from frequency calculations using a scaling factor of 0.9735 to account for anharmonicity.<sup>52</sup> Single-point calculations were performed with a more flexible basis set (B1B95/6-311++G(3df,2p)/B1B95/6-31+G\*\*) and also estimating the effect of the aqueous solution with a polarizable continuum model<sup>55</sup> (PCM/B1B95/6-31+G\*\*//B1B95/6-31+G\*\*). The nature of the ground (zero imaginary frequency) and transition (one imaginary frequency) states was verified by frequency calculations. The B3LYP method employing a triple- $\zeta$  basis set (B3LYP/6-311G\*\*//B1B95/6-31+G\*\*) was used to compute molecular properties since this HDFT method was found by us to provide reliable hyperfine coupling constants<sup>31,56–58</sup> and optical transitions<sup>30a,31</sup> in nucleosides. In Figures 6 and 8, and Tables S1 and S2, we have reported the electronic transitions having an oscillator strength  $f$  greater than 0.01.

**Acknowledgment.** Work supported in part by the European Community's Marie Curie Research Training Network under Contract MRTN-CT-2003-505086 [CLUSTOXDNA]. We thank Professor M. Orfanopoulos (University of Crete) for some helpful discussions and for allowing GCV to visit Bologna during his PhD work. We thank A. Monti and A. Martelli for assistance with pulse radiolysis experiments.

**Supporting Information Available:** Pulse radiolysis experiments, product studies, DFT calculations, and the full citation for ref 51. This material is available free of charge via the Internet at <http://pubs.acs.org>.

JA062636H

- (43) (a) Holmes, R. E.; Robins, R. K. *J. Am. Chem. Soc.* **1964**, *86*, 1242. (b) Lin, T. S.; Cheng, J. C.; Ishiguro, K.; Sartorelli, A. C. *J. Med. Chem.* **1985**, *28*, 1194.
- (44) Saneyoshi, M. *Chem. Pharm. Bull.* **1968**, *16*, 1616.
- (45) Yamauchi, K.; Tabnabe, T.; Kinoshita, M. *J. Org. Chem.* **1979**, *44*, 638.
- (46) Sako, M.; Kawada, H.; Hirota, K. *J. Org. Chem.* **1999**, *64*, 5719.
- (47) (a) Buxton, G. V.; Mulazzani, Q. G. In *Electron Transfer in Chemistry*; Balzani, V., Ed.; Wiley-VCH: Weinheim, Germany, 2001; Vol. 1, p 538. (b) Spinks, J. W. T.; Woods, R. J. *An Introduction to Radiation Chemistry*, 3rd ed.; Wiley: New York, 1990; p 100.
- (48) Becke, A. D. *Phys. Rev. A* **1988**, *38*, 3098.
- (49) Becke, A. D. *J. Chem. Phys.* **1996**, *104*, 1040.
- (50) Zhao, Y.; Pu, J.; Lynch, B. J.; Truhlar, D. G. *Phys. Chem. Chem. Phys.* **2004**, *6*, 673.
- (51) Frisch, M. J., et al. *Gaussian 03*, revision B.5; Gaussian, Inc.; Pittsburgh, PA, 2003.
- (52) Zhao, Y.; Lynch, B. J.; Truhlar, D. G. *J. Phys. Chem. A* **2004**, *108*, 2715.
- (53) Zhao, Y.; Truhlar, D. G. *J. Phys. Chem. A* **2004**, *108*, 6908.

- (54) (a) Guerra, M. *Chem. Phys. Lett.* **1990**, *167*, 315. (b) Guerra, M. *J. Phys. Chem. A* **1999**, *103*, 5983.
- (55) Cossi, M.; Scalmani, G.; Rega, N.; Barone, V. *J. Chem. Phys.* **2002**, *117*, 43.
- (56) Chatgililoglu, C.; Gimisis, T.; Guerra, M.; Ferreri, C.; Emanuel, C. J.; Horner, J. H.; Newcomb, M.; Lucarini, M.; Pedulli, G. F. *Tetrahedron Lett.* **1998**, *39*, 3947.
- (57) Guerra, M. *Phys. Chem. Chem. Phys.* **2001**, *3*, 3792.
- (58) Guerra, M. *Res. Chem. Intermed.* **2002**, *28*, 257.